Technical report on physical wave modeling and hypothetical offshore sand borrow sites

Prepared for

BOEM-NYS DOS Cooperative Agreement M14AC00001

Prepared by

Robert Wilson, Amin Ilia, Henry Bokuniewicz and Claudia Hinrichs
School of Marine and Atmospheric Sciences
Stony Brook University
Stony Brook, NY 11794-5000

2016

Stony Brook University's COAST Institute

The Coastal Ocean Action Strategies (COAST) Institute was created in 1989 within the School of Marine and Atmospheric Sciences to assist in coastal zone management and coastal marine policy analysis. We do this by exploring future scenarios for Long Island's coastline and coastal environment and by working with policy makers and environmental managers in identifying and analyzing strategies that will conserve and, when necessary, rehabilitate the coastal ocean; by ensuring that not only is the best technical information included in developing the strategies, but economic and other critical information as well; and by forming effective linkages among environmental groups, the scientific community, lawmakers, regulators, and managers to tackle coastal environmental issues.

COAST has been called upon to assist in resolving coastal problems at home on Long Island, throughout the U.S. and in many parts of the world. COAST also provides a real world, action-learning laboratory for graduate students at MSRC. Each year students who are interested in coastal management and policy take part in gathering and analyzing data, in transforming data into information, and in synthesizing information-all targeted at identifying and evaluating management alternatives to attack the problems that COAST is helping to solve.

Technical report on physical wave modeling and hypothetical offshore sand borrow sites

Robert Wilson, Amin Ilia, Henry Bokuniewicz and Claudia Hinrichs
School of Marine and Atmospheric Sciences
Stony Brook University
Stony Brook, NY 11794-5000

May 2016

INTRODUCTION

Marine sand deposits on the Outer Continental Shelf have been used for a variety of purposes, including shoreline protection efforts, coastal restoration, reconstruction, beach nourishment, breach fills, and sand stockpiling. In order to examine the potential impacts of sand extraction, we conducted physical wave modeling to assess the effects of potential sediment borrow areas on nearshore wave climate and longshore sediment transport. Results should lead to the identification of those borrow area locations which might have minimal effect, and those locations which might have a more detrimental effect on wave climate and longshore transport. We are primarily concerned at this stage with the transport of sand along the shore. The magnitude of longshore transport depends on the wave height and the angle at which the waves approach the shore. Both of these characteristics are changed by the presence of borrow areas. If the changes are such that more sand is moved out of a stretch of beach than moves into it, the beach will erode as a result of the borrow area. The changes may result in more sand moving into a stretch of beach and subsequent accretion. To address the cross-shore transport of sand, models of advective currents, like the tides, would have to be combined with wave model results. The wave modeling conducted here is limited in the sense that it involves the wave model SWAN forced by offshore storm waves with characteristics determined by wave climatology defined at offshore buoys, and it does not include wave-current interaction.

Background

As reported by Dalyander et al. (2015), similar studies in other areas have shown that impacts of borrow areas are quite site-specific and depend on details in the bathymetry. Dalyander et al. (2015) emphasized that borrow areas are perturbations to shallow-water bathymetry which can modify the nearshore wave field. These modifications can alter the longshore sediment transport rates and patterns and produce new erosional or accretional patterns along the beach. Dalyander et al. (2015) analyzed the effects of proposed sediment borrow areas on nearshore wave climate and longshore sediment transport rate along Breton Island, Louisiana using the spectral wave model SWAN (http://www.swan.tudelft.nl/), and a volumetric longshore sediment transport relation based on wave energetics (Longuet-Higgins, 1972).

As part of a regional MMS effort, Byrnes et al. (2004) specifically examined the potential physical and environmental impacts of sand extraction from ridges and shoals at three potential sites in Federal waters off the coast of New York south of Long Beach and Jones Beach on Long Island. Ridges in these areas range from 2 to 4 m above the sea floor and water depths over the ridges range from 17 to 20 m. In assessing physical impacts of dredging, Byrnes et al. (2004) assumed ridges at the three sites would be excavated to the elevation of the ambient sea floor. Byrnes et al. (2004) used numerical modeling techniques to examine potential impacts this removal of sand would have on the wave characteristics and sediment transport patterns in the vicinity of the borrow areas and on the adjacent shorelines. They employed the spectral wave model REF/DIF S (http://coastal.udel.edu/~fyshi/refdifwin/refdifwin.html) to analyze how the borrow areas would change wave characteristics associated with dominant wave directional conditions. They developed numerical techniques to use wave information from REF/DIF S with a wave-induced current model (Winer, 1988; Ramsey, 1991) to evaluate longshore sediment transport patterns.

Study Objectives

The specific objectives of the present study are to assess the effects of hypothetical sediment borrow areas located in Federal waters off the south shore of Long Island, as shown in Figure 1, on:

1. Nearshore wave climate: significant wave height, wave direction, wave energy.
2. Longshore sediment transport rates and transport patterns in the littoral system.

These locations were chosen for modeling in part due to proximity to coastal areas where sand demand for various projects is expected to be high. The sites were spaced relatively equidistantly to represent various conditions along the south shore of Long Island. This assessment may lead to the identification of those borrow area locations which might have minimal effect, and those locations which might have a more detrimental effect on wave climate and longshore transport and ultimately on erosional or accretional patterns along the shore. As discussed below, we choose to use the contemporary community spectral wave model SWAN and an easily applied longshore sediment transport relation based on wave energetics (Longuet-Higgins, 1972).

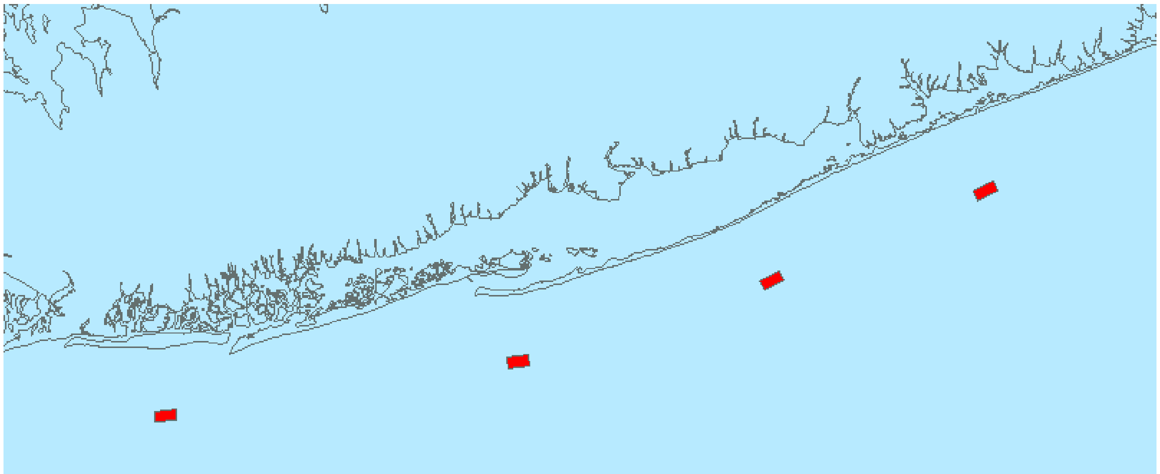

Figure 1. Hypothetical borrow sites in federal waters off the south shore of Long Island (see Table 1), distributed (from west to east) off the coasts of Long Beach, Fire Island Inlet, Fire Island, and West Hampton.

METHODS

For this assessment we are following basic methods outlined by Dalyander et al. (2015) and Long et al. (2014). This involves:

1. Defining offshore wave climatology by analyzing long term records from regional wave buoys. In our case NOAA/NDBC wave buoys 44025 and 44017 are most relevant.
2. In light of this wave climatology, identifying those waves expected to most influence coastal wave climate and longshore sand transport in terms of significant wave height, wave direction, and wave period. Longshore sand transport is highly sensitive to significant wave height Hs varying as Hs to the 5/2 power. It is also sensitive to wave direction; see equations (1) and (2).
3. Creating boundary conditions in the SWAN model that generate the representative waves identified in Step 2 for the domain shown in Figure 2. Exercise SWAN for existing bathymetry and shoreline orientation shown in Figure 2 and described below, and for bathymetries modified to represent borrow areas described below in (Table 1).
4. Using wave model output, diagnose changes in: a) coastal wave climate as represented by significant wave height, wave direction and wave energy dissipation due to breaking, and b) longshore sand transport rate.
5. Following Dalyander et al. (2015), using the changes in the divergence in longshore sand transport to infer possible changes in coastal erosion or accretion.

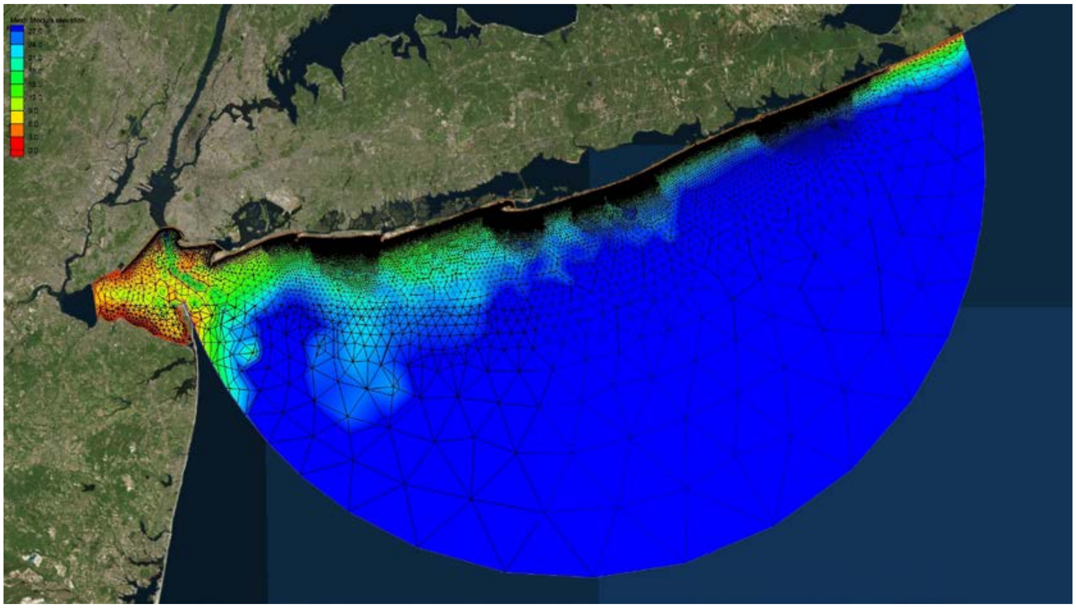

Figure 2. Swan wave model domain and unstructured grid.

Wave Climatology

Wave characteristics were derived from the National Data Buoy Center (NDBC) buoys 44025 and 44017. Buoy 44025 http://www.ndbc.noaa.gov/station_page.php?station=44025 is located 30 nautical miles south of Islip, NY (40.251 N 73.164 W) (656149.55 Easting 4457233.21 Northing) in water 40.8 m deep.

Buoy 44017 http://www.ndbc.noaa.gov/station_page.php?station=44017 is located 23 nautical miles south southwest of Montauk Point, NY (40.694 N 72.048 W) (749429.09 Easting 4508980.66 Northing) in water 52.4 m deep.

Histograms constructed from observations at NDBC buoy 44025 (Figures 3 and 4) emphasize that waves, presumably storm induced, with significant wave heights (Hs) greater than 4 m come from a distinctly different direction than waves with Hs less than 4 m, and they have a distinctly different period. The median wave direction wave for these larger waves is 109° and the median wave period is 7.3 s. Because of their large amplitude and median period (7.3 s), we conclude that these larger waves are primarily sea waves rather than swell. The median wave direction wave for waves with Hs less than 4 m is 156° and the median wave period is 4.8 s. These smaller, shorter period waves are certainly sea waves.

Histograms for NDBC buoys 44017 and 44025 (Figures 5 and 6) show frequency of occurrence (percent) of waves as function of significant wave height and mean wave direction. They emphasize the dominance of waves with Hs less than 1.5 m with directions consistent with those shown in Figure 3.

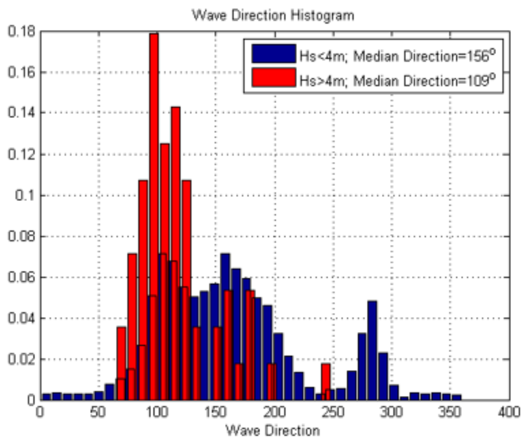

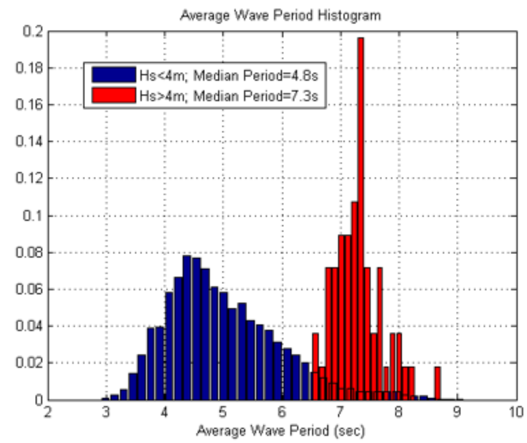

Figure 3. Wave direction histogram 44025. **Figure 4.** Wave period histogram 44025.

For 7.3 second waves in water ranging from 20 m to 50 m in depth, the wavelength varies from 78 m to 85 m. The wavelength for 4 second waves is approximately 25 m. The large amplitude, long period and longer wavelength waves should be markedly more sensitive to topographic changes through refraction and shoaling processes than the shorter waves. We elected to diagnose the wave response to borrow areas for these large amplitude, long period, long wavelength waves from a more easterly direction, rather than for a mixed wave field which includes shorter period sea waves.

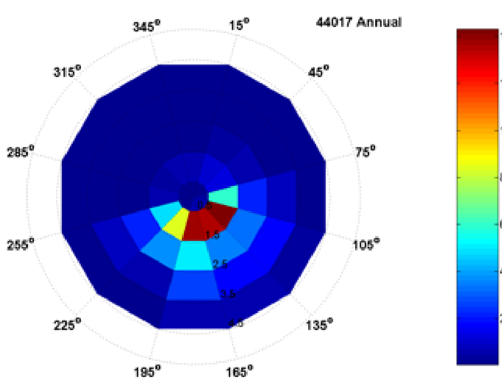

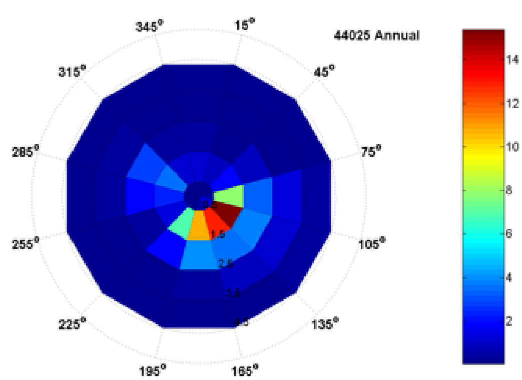

Figure 5. Wave direction histogram 44017. **Figure 6.** Wave direction histogram 44025

Numerical Wave Model SWAN

SWAN is a numerical wave model capable of predicting nearshore wave conditions from offshore wave characteristics. SWAN forecasts the transformations waves undergo as they move into shallower water, specifically it was designed to "…estimate wave conditions in small-scale, coastal regions with shallow water, barrier islands, tidal flats, local wind, and ambient currents." (Ris et al.1999). SWAN has been applied successfully in coastal settings including: Lake Okeechobee (Jin and Ji 2001), a portion of the Rhine estuary(Ris et al. 1999), off the outer banks of North Carolina, and the on the Pacific shelf off of Washington (Palmsten, 2001*)* as well as Long Island's south shore (Buonaiuto et al. 2011).

SWAN accounts for variations in wind energy, refraction, energy dissipation due to white - capping, bottom friction, depth-induced breaking, and nonlinear wave-wave interactions (Booij et al. 1999). Booij et al. (1999) provided the first validation of SWAN. In initial tests, SWAN calculations closely matched observed experimental data (Booij et al. 1999). The link to the version of SWAN used in these simulations is http://swanmodel.sourceforge.net/.

Calculations are done on an unstructured grid with the domain shown in Figure 2 which has a resolution of approximately 100 m in the band between the limit of State waters three nautical miles offshore and the 30-meter bathymetric contour. The bathymetry data used in these simulations is provided by National Centers for Environmental Information, U.S. Coastal Relief Model (http://www.ngdc.noaa.gov/mgg/coastal/crm.html). These data are constantly updated and the retrieval date for the data used in this analysis was February 2016. These data are interpolated to the unstructured grid shown in Figure 2; they should provide a good representation of existing bathymetric features including offshore sand ridges.

As explained in the previous section on wave climatology developed from offshore buoys, we elected to diagnose the response to borrow areas for the large amplitude, long period, long wavelength from a specific direction, rather than for a mixed wave field. This type of forcing allows us to diagnose changes in refraction patterns, changes in Hs and changes in patterns of wave breaking more clearly than for a mixed wave field. Specifically, we forced on the boundary climatologically distinct waves with Hs=4.0 m, Tp=7.4 s and for incident direction 110^{o}. For each proposed borrow site, simulations were run first for existing bathymetry, and then for the modified bathymetry. Finally, differences in wave properties were analyzed. In addition, and only to provide a comparison with waves from an alternative direction, we did very limited simulations for waves from a more southerly direction: Hs=4.0 m, Tp=7.4 s for incident direction 170^{o}.

Borrow Area Design

Wave simulations were performed to diagnose the effects of four borrow areas distributed from west to east: Long Beach, Fire Island Inlet, Fire Island and West Hampton (Figure 1). Table 1 lists the UTM coordinates for each area. The dimension of each area is approximately 2km × 1km; the depth of the area was taken to be 3 m below the ambient depth. The ambient depths are shallowest in the vicinity of the Long Beach borrow area and we expect that these shallow depths would produce more changes in wave properties than areas at the other sites.

Table 1. Borrow Area coordinates (UTM)

Borrow Area ID	Corner	Easting	Northing
Long Beach	Top Left	613677.8	4487460.3
Long Beach	Bottom Left	613751.9	4486462.3
Long Beach	Top Right	615669.6	4487605.3
Long Beach	Bottom Right	615745.8	4486610.4
FI Inlet	Top Left	646163.5	4492378.3
FI Inlet	Bottom Left	646309	4491399.4
FI Inlet	Top Right	648134.7	4492677.3
FI Inlet	Bottom Right	648285.5	4491690.4
Fire Island	Top Left	664614.2	4497637.8
Fire Island	Bottom Left	664995.2	4496711.7
Fire Island	Top Right	666461	4498394.5
Fire Island	Bottom Right	666842	4497471.1
West Hampton	Top Left	703607.5	4514645
West Hampton	Bottom Left	704052	4513758.7
West Hampton	Top Right	705393.5	451534.01
West Hampton	Bottom Right	705838	4514642.4

RESULTS

Changes in Hs and Wave Direction

Results for wave properties from simulations at each borrow area were diagnosed along cross-shore transects; Figure 7 shows the Long Beach borrow area region. As an example, Figures 8 and 9 show the horizontal patterns of the local changes in Hs and wave direction associated with the introduction of the borrow area for simulations with Hs=4.0 m, Tp=7.4 s and wave direction 170°. These changes were calculated as Hs with the area minus Hs without the area. These figures emphasize that the Hs difference is confined to within approximately 2 km of the borrow area with maximum value of the order 0.1 m. They also emphasize that wave direction difference is localized in the vicinity of the borrow area with maximum value on the order of 3°. Changes in Hs and wave direction for simulations with Hs=4.0 m, Tp=7.4 s and boundary wave direction 110° are similar showing primarily localized changes.

Waves from direction 110°, of course, undergo more refraction than waves from 170°. Simulations for wave directions 110° and 170° both show very small fractional changes in wave breaking energy inshore of the borrow area.

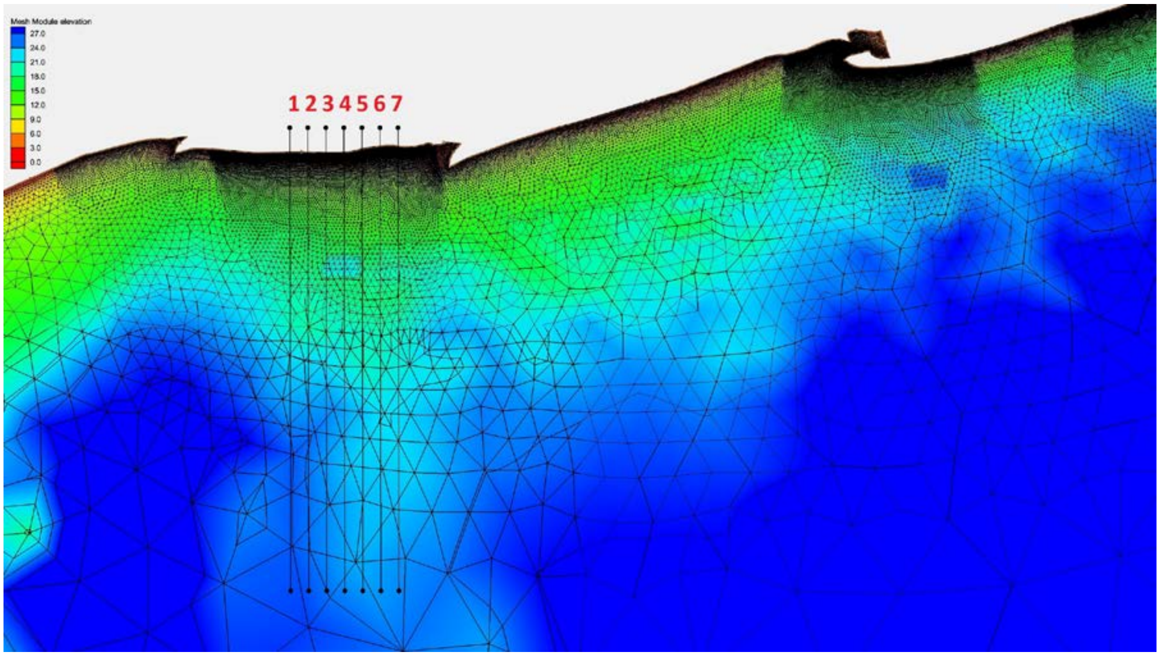

Figure 7. Swan wave unstructured grid and transects through Long Beach borrow area.

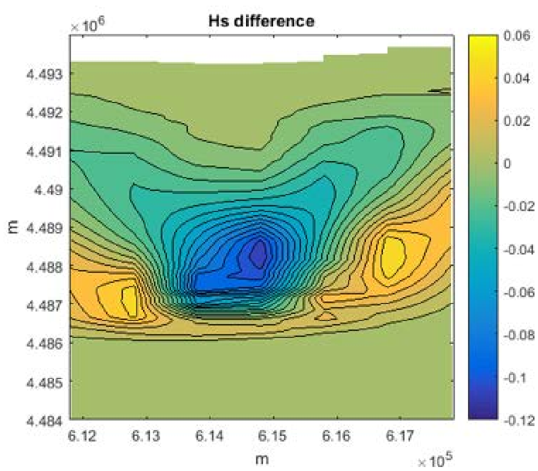

Figure 8. Hs difference at Long Beach.

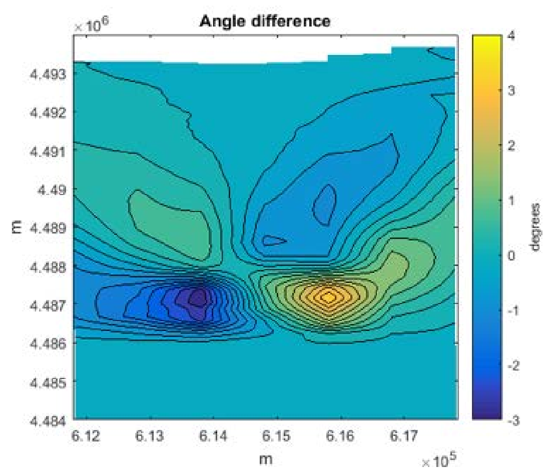

Figure 9. Angle difference at Long Beach.

Changes in Longshore Volumetric Transport and Transport Divergence

Following Dalyander et al. (2015) we estimate the cross-shore integrated volumetric sediment transport rate for sand-sized sediment as:

$$Q_l = \frac{0.8P_l}{(\rho_s - \rho_w)g(1-n)} \qquad (1)$$

where ρ_s (2.65×10^3 kgm^{-3}) and ρ_w (1.024×10^3 kgm^{-3}) are the densities of sand and water and n is sediment porosity (0.4). P_l is the longshore component of wave energy flux given by (Dean and Dalrymple, 2002):

$$P_l = 0.0884 \rho_w g^{3/2} H_b^{5/2} \sin\alpha_b \cos\alpha_b \qquad (2)$$

where H_b is breaking wave height approximated by Hs/1.4, and α_b is incident breaking wave angle relative to the shoreline. Dalyander et al. (2015) evaluated the breaking wave height and direction at the offshore location where the energy dissipation due to depth-induced breaking first exceeded 0.01 W/m2. Figure 10 shows energy dissipation due to wave breaking along all seven transects in Figure 7. It emphasizes that the choice of this threshold is likely very conservative and that a higher threshold would place the cross-shore location defining H_b and α_b further inshore at distance from the borrow area.

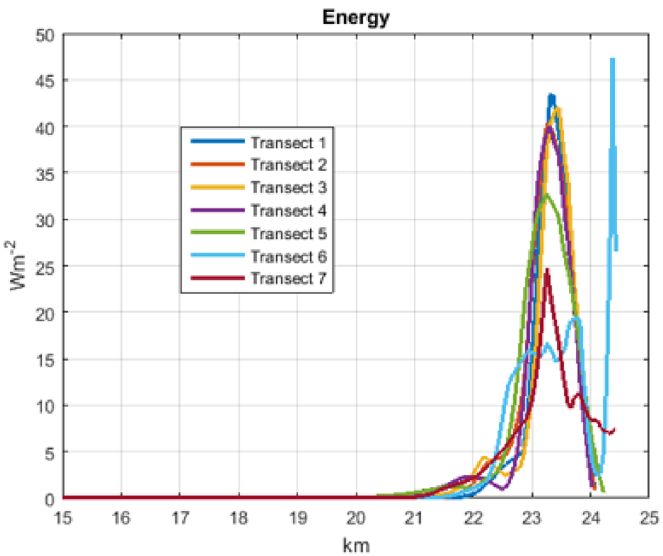

Figure 10. Wave breaking energy as a function of cross-shore distance at Long Beach..

Estimates of Q_l based on expression (1) for simulations with Hs=4.0 m, Tp=7.4 s and wave direction 110^o are shown in Figures 11 and 12 for the shallow Long Beach sections and the deeper West Hampton sections, respectively. Note that these units are m^3/s; to convert to more common unit for longshore transport m^3/yr one must consider the fraction of occurrence of these waves during the year which is approximately 0.008 or 0.8% (see Dalyander et al., 2015). Estimates for cross-shore integrated longshore sediment transport rates at both Long Beach and West Hampton are of the order 2.6×10^5 m^3/yr. The borrow areas seem to cause only very small changes.

The longshore divergence in volumetric transport $\Delta Q_l/\Delta x$ (Figures 13 and 14) is of the order 10^{-4} m^2/s at both Long Beach and West Hampton where Δx is 10^3 m. A positive $\Delta Q_l/\Delta x$

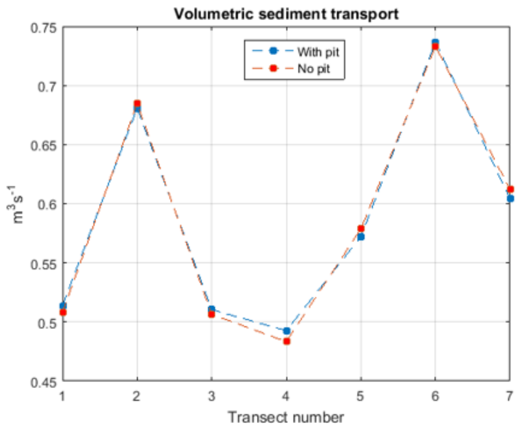

Figure 11. Q_l at Long Beach.

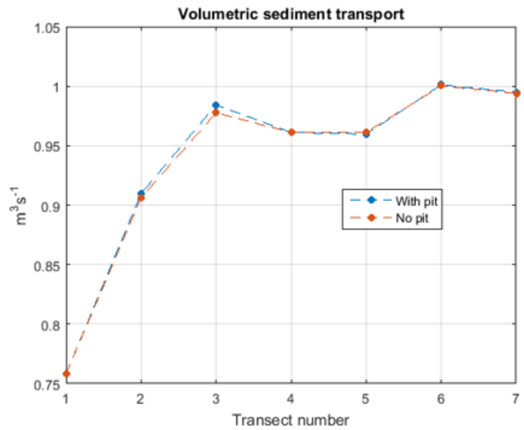

Figure 12. Q_l at West Hampton.

means that more sand is entering the beach section between the transects than leaving it, and the beach will widen. A negative value means that more sand is leaving the beach section between the transects, and the beach will erode. A common empirical, engineering expedient is the "rule-of-thumb" that one cubic yard of sand is needed to widen the beach by one foot along every foot of shoreline. This implies that a $\Delta Q_l/\Delta x$ of the order 10^{-4} m^2/s (Figures 13 and 14) would correspond to a change in the width of the beach between two transects of 10 feet in one year.

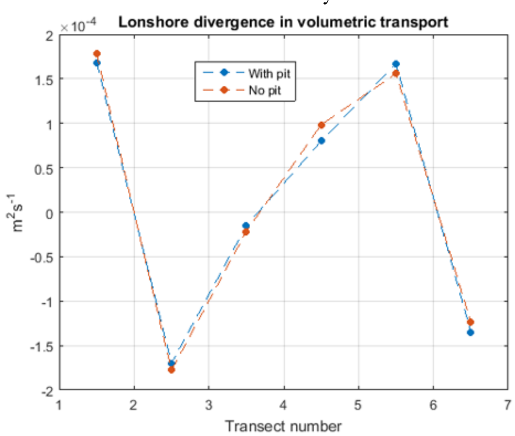

Figure 13. $\Delta Q_l/\Delta x$ at Long Beach

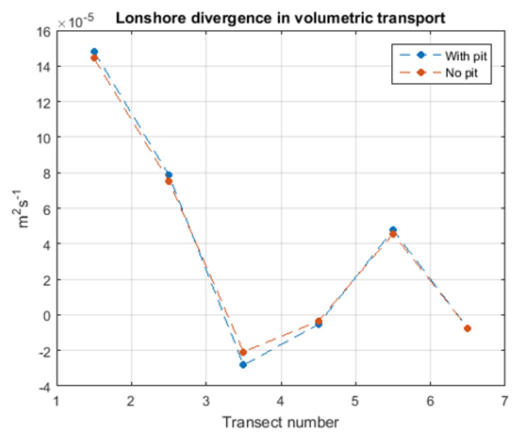

Figure 14. $\Delta Q_l/\Delta x$ at West Hampton.

The gradient in the longshore transport was calculated in the current conditions and again recalculated in the presence of a hypothetical borrow area. If the longshore gradient after the area is in place is less than (below) that value before the area is in place, erosion is made worse by the presence of the area. Alternatively, if the longshore gradient after the area is in place is greater than (above) that before, the erosion is lessened by the presence of the area (or accretion is enhanced). Although the changes in Figures 13 and 14 are quite small, Figure 15 associated with simulations for Hs=4.0 m, Tp=7.4 s and wave direction 170° show a significant change at Long Beach. So wave direction can be important; in order to estimate the net effect on the shoreline over the course of a year, the full suite of realized waves would need to be modelled taking into account the fraction of time that they were present.

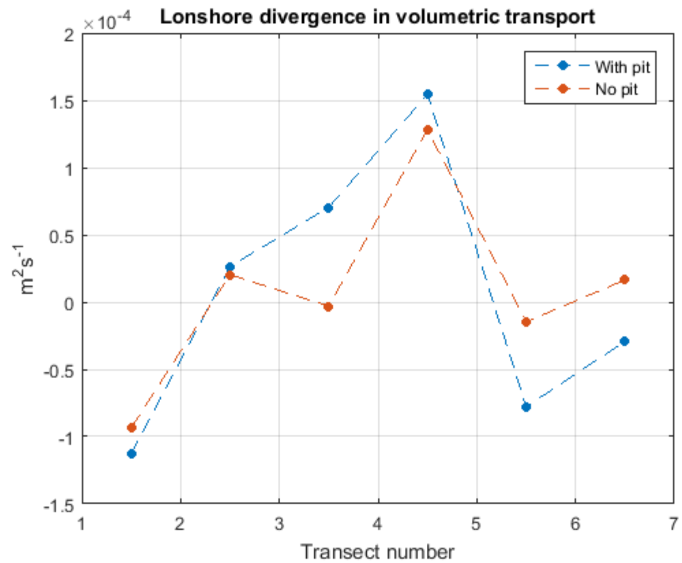

Figure 15. $\Delta Q_l/\Delta x$ at Long Beach for wave angle 170°.

CONCLUSIONS

Observable effects of the borrow area on changes in Hs and on wave direction are confined to within approximately 2 km in the vicinity of the area. Even long period sea waves tend to break well inshore of the modeled borrow area location which is three miles offshore. Simulations point to some possible divergence in volumetric transport inshore of the borrow area based on the conservative threshold of 0.01 W/m^2 to define H_b and α_b. A less conservative threshold would imply a reduction in transport divergence. In the worse-case scenario (Long Beach), the changes at the shoreline are relatively small and unlikely to be detectable among the natural variations. It should be emphasized that these are very limited model simulations; to estimate the net effect of the offshore wave field on the shoreline over the course of a year, a full suite of realized waves and additional factors affecting sand transport would need to be taken into account.

REFERENCES

Byrnes, M.R., R. M. Hammer, T.D. Thibaut, and D.B.Snyder, 2004. Effects of Sand Mining on Physical Processes and Biological Communities Offshore New Jersey, U.S.A. Journal of Coastal Research 20: 25-43.

Booij, N, R.C. Ris, L.H. Hothuijsen. 1999. A third-generation wave model for coastal regions 1. Model description and validation. Journal of Geophysical Research. 104(C4): 7649-7666.

Buonaiuto, F.S. Jr,, M.Slattery and H. J. Bokuniewicz, 2011. Wave Modeling of Long Island Coastal Waters, Journal of Coastal Research 27; 470-477 doi: 10.2112/08-1014.

Dalyander, P.S., Mickey, R.C., Long, J.W., and Flocks, James, 2015. Effects of proposed sediment borrow pits on nearshore wave climate and longshore sediment transport rate along Breton Island, Louisiana: U.S. Geological Survey Open-File Report 2015–1055, 41 p., http://dx.doi.org/10.3133/ofr20151055.

Dean, R.G. and R.A. Dalyrmple. 2002. Coastal Processes with Engineering Applications. Cambridge University Press, New York, 475 pp.

Jin, Kang-Ren, Zhen-Gang Ji. 2001. Calibration and verification of the spectral wind-wave model for Lake Okeechobee. Ocean Engineering. 28: 571-584.

Long, J.W., N.G. Plant, P.S. Dalyander, and D.M. Thompson, 2014. A probabilistic method for constructing wave time-series at inshore locations using model scenarios, Coastal Engineering 89: 53–62 doi:10.1016/j.coastaleng.2014.03.008

Ramsey, J.S., 1991. A Study of Wave-Induced Currents Behind Shore Parallel Breakwaters. Newark, Delaware: M.C.E. Thesis, Department of Civil Engineering, University of Delaware, 101pp.

Ris, R.C., L.H. Holthuijsen, N. Booij. 1999. A third-generation wave model for coastal regions 2. Verification. Journal of Geophysical Research. 104(C4: 7667-7681.

Palmsten, M.L. 2001. Application of the SWAN wave model to a high-energy continental shelf. MA thesis University of South Florida.

Rogers, W.E., J.M. Kaihatu, H.A.H. Petit, N. Booij, L.H. Holthuijsen. 2002. Diffusion reduction in an arbitrary scale third generation wind wave model. Ocean Engineering. 29: 1357-1390.

Rogers, W.E., P.A. Hwang, D.W. Wang. 2003. Investigation of wave growth and decay in the SWAN model: three regional-scale applications. Journal of Physical Oceanography. 33: 366-389.

Winer, H., 1988. Numerical Modeling of Wave-Induced Currents Using a Parabolic Wave Equation. Gainesville, Florida: Department of Coastal and Oceanographic Engineering, University of Florida, Technical Report No. 80.

APPENDIX I. Fire Island Inlet Borrow Area

SWAN results for Hs=4.0 m, Tp=7.4 s and wave direction 110° presented as transect plots for bathymetry, Hs, wave angle and wave breaking energy. Transect plots show that the borrow area produces some changes to Hs and wave angle in the immediate vicinity of the area. Wave breaking occurs far inshore of the borrow area where there is little discernible change in either Hs or wave angle. According to equations (1) and (2) this would suggest that the area produces minimal change in long-shore sediment transport for these waves.

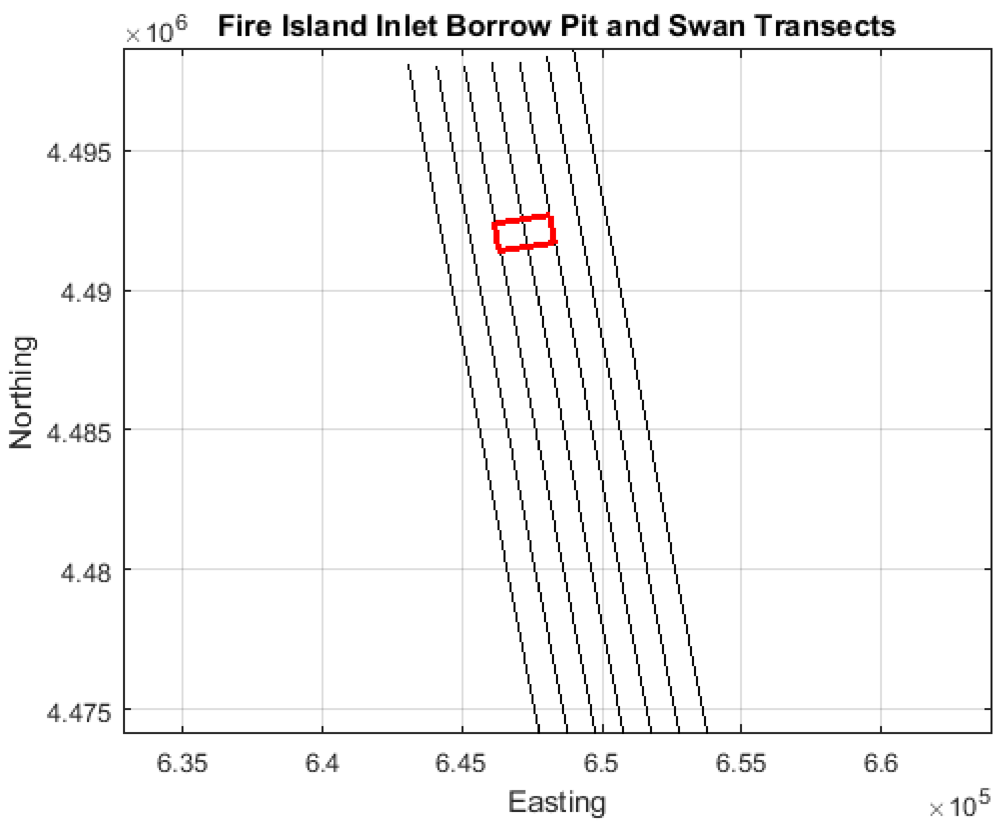

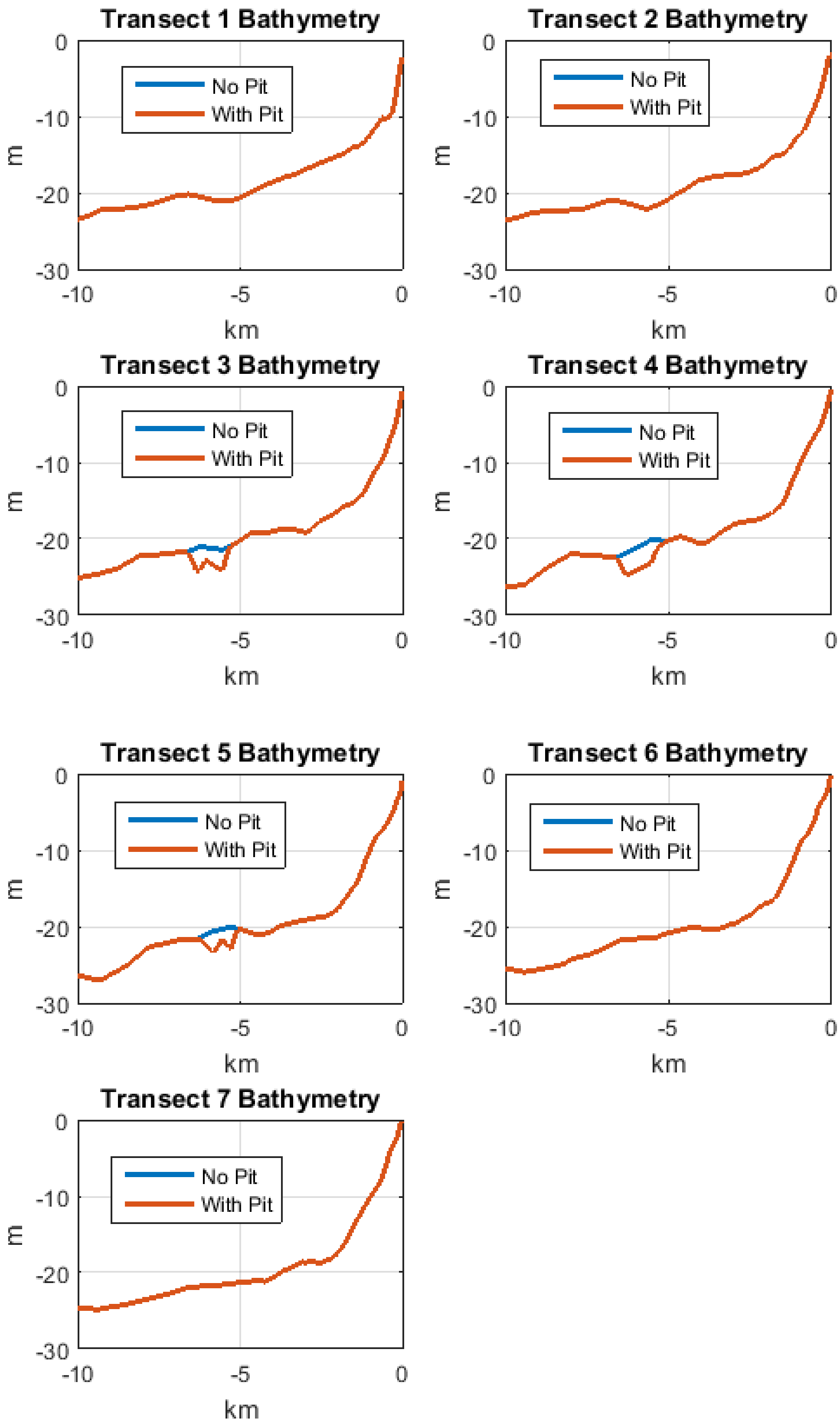
Transect 1 Bathymetry
Transect 2 Bathymetry
Transect 3 Bathymetry
Transect 4 Bathymetry
Transect 5 Bathymetry
Transect 6 Bathymetry
Transect 7 Bathymetry
No Pit
With Pit
m
km
0
-10
-20
-30
-5

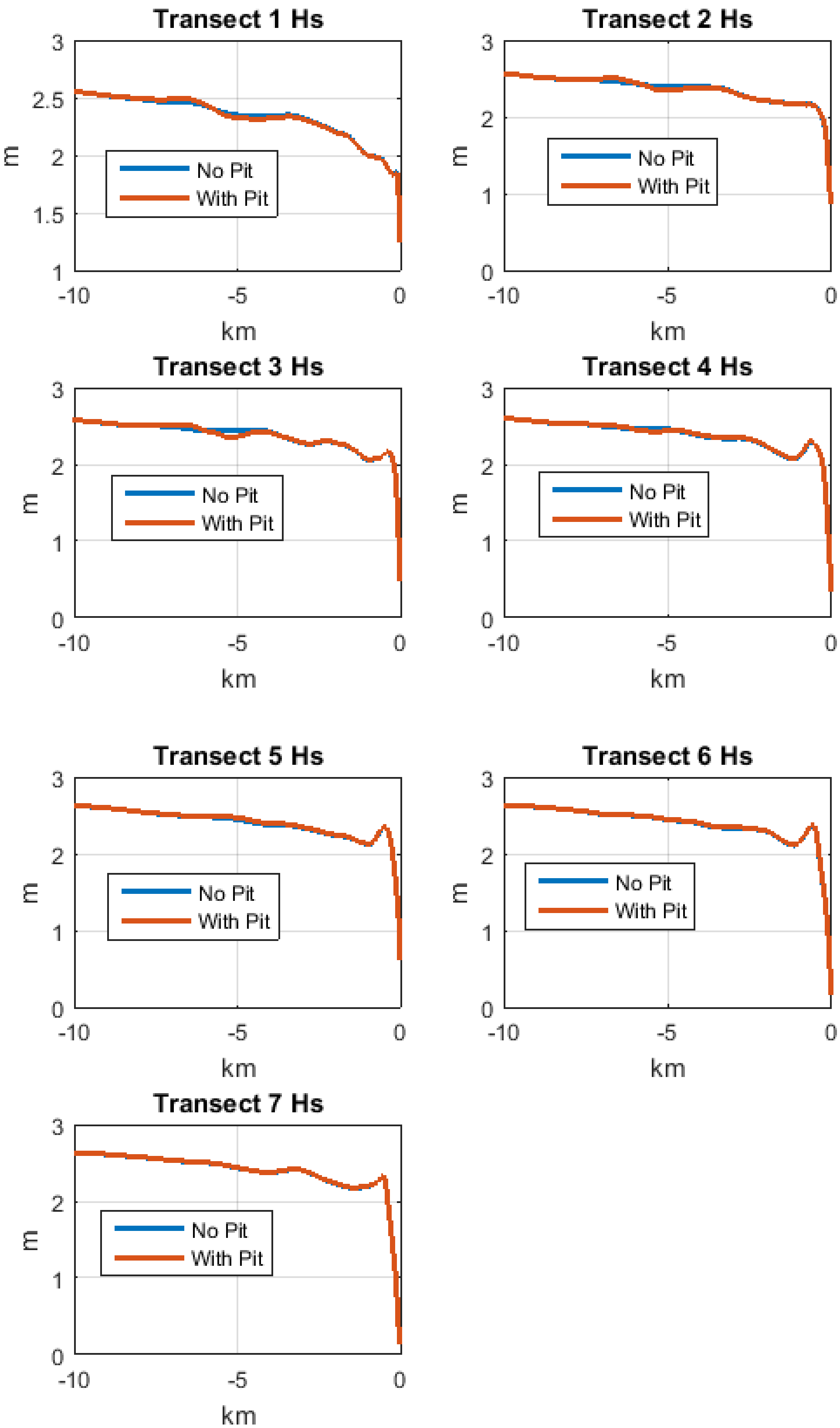
Transect 1 Hs
Transect 2 Hs
Transect 3 Hs
Transect 4 Hs
Transect 5 Hs
Transect 6 Hs
Transect 7 Hs
No Pit
With Pit
m
km

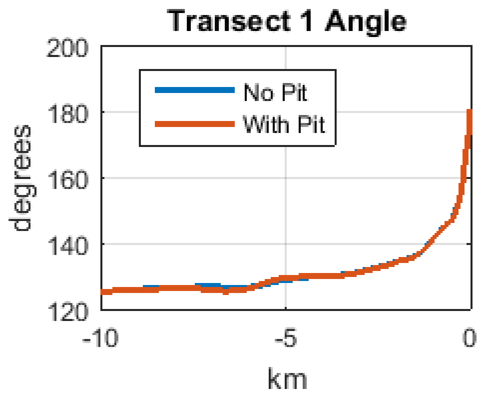
Transcect 1 Angle
200
180
160
140
120
degrees
No Pit
With Pit
-10
-5
0
km

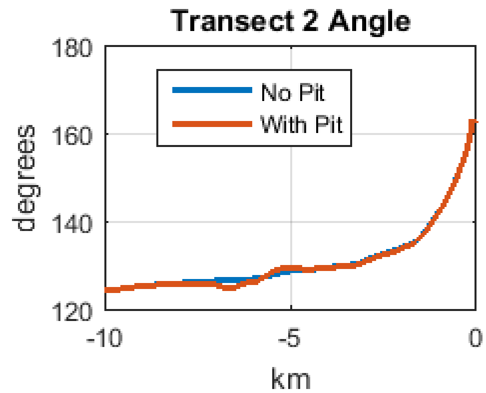
Transcect 2 Angle
180
160
140
120
degrees
No Pit
With Pit
-10
-5
0
km

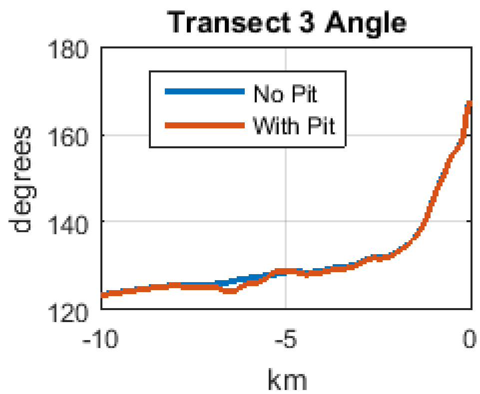
Transcect 3 Angle
180
160
140
120
degrees
No Pit
With Pit
-10
-5
0
km

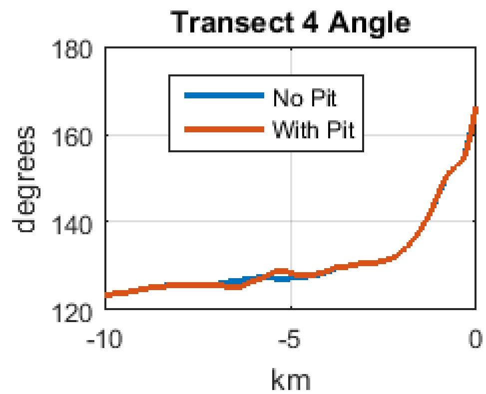
Transcect 4 Angle
180
160
140
120
degrees
No Pit
With Pit
-10
-5
0
km

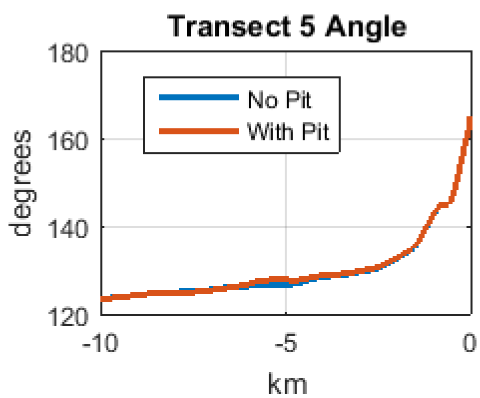
Transcect 5 Angle
180
160
140
120
degrees
No Pit
With Pit
-10
-5
0
km

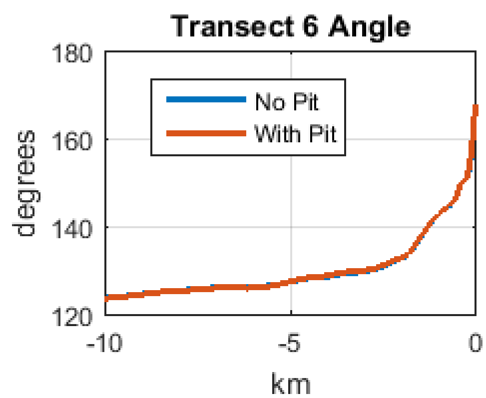
Transcect 6 Angle
180
160
140
120
degrees
No Pit
With Pit
-10
-5
0
km

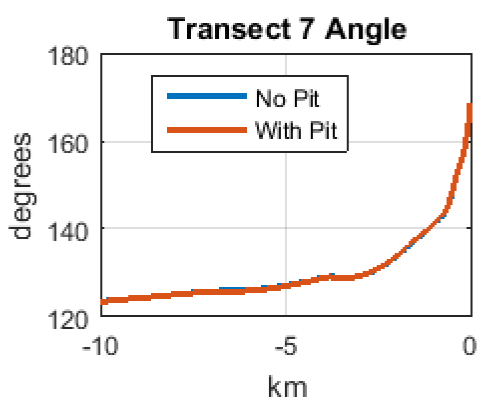
Transcect 7 Angle
180
160
140
120
degrees
No Pit
With Pit
-10
-5
0
km

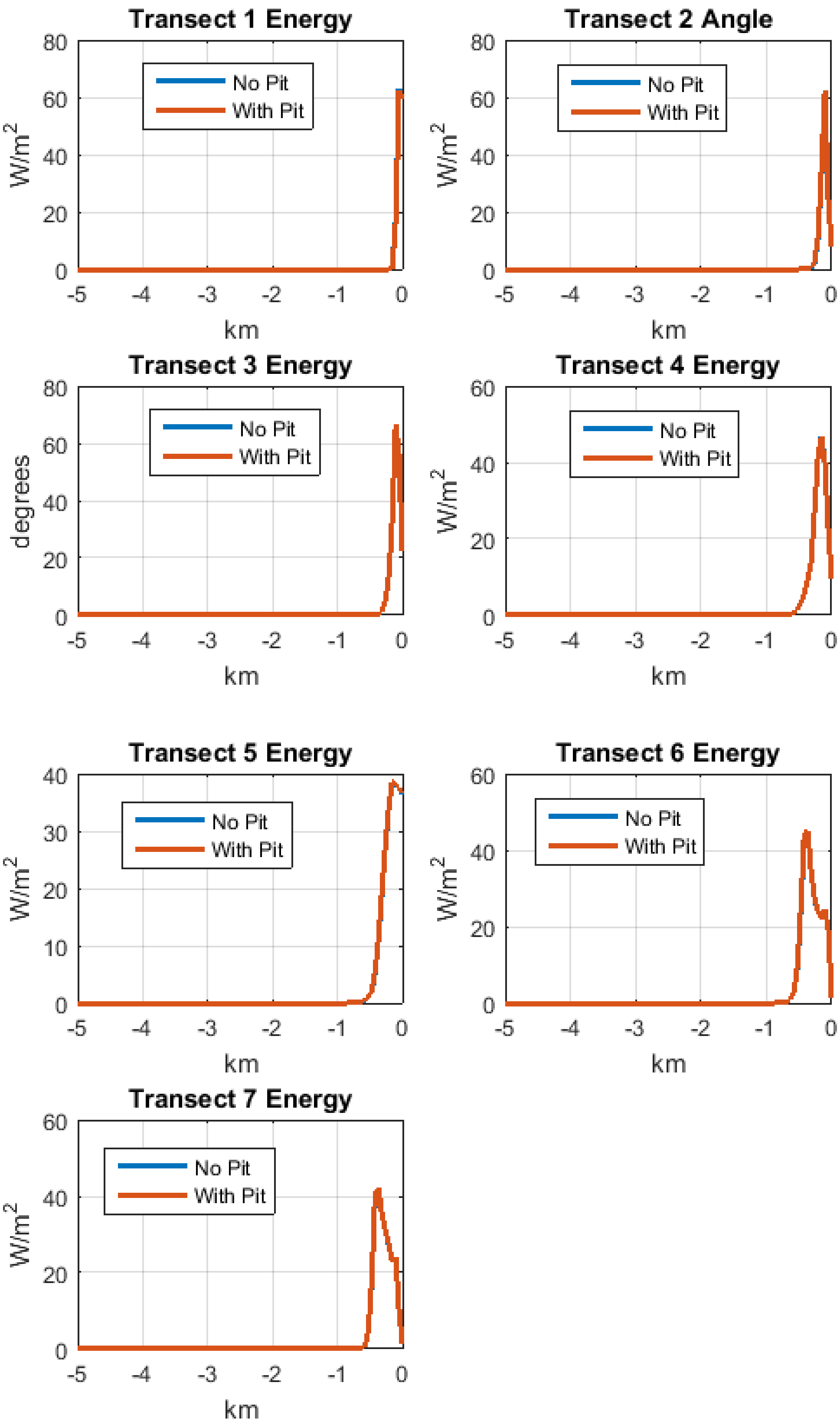

Transect 1 Energy
W/m2
km
No Pit
With Pit
Transect 2 Angle
W/m2
km
No Pit
With Pit
Transect 3 Energy
degrees
km
No Pit
With Pit
Transect 4 Energy
W/m2
km
No Pit
With Pit
Transect 5 Energy
W/m2
km
No Pit
With Pit
Transect 6 Energy
W/m2
km
No Pit
With Pit
Transect 7 Energy
W/m2
km
No Pit
With Pit

APPENDIX II. Fire Island Borrow Area

SWAN results for Hs=4.0 m, Tp=7.4 s and wave direction 110° presented as transect plots for bathymetry, Hs, wave angle and wave breaking energy. Transect plots show that the borrow area produces some changes to Hs and wave angle in the immediate vicinity of the area. Wave breaking occurs far inshore of the borrow area where there is little discernible change in either Hs or wave angle. According to equations (1) and (2) this would suggest that the area produces minimal change in long-shore sediment transport for these waves.

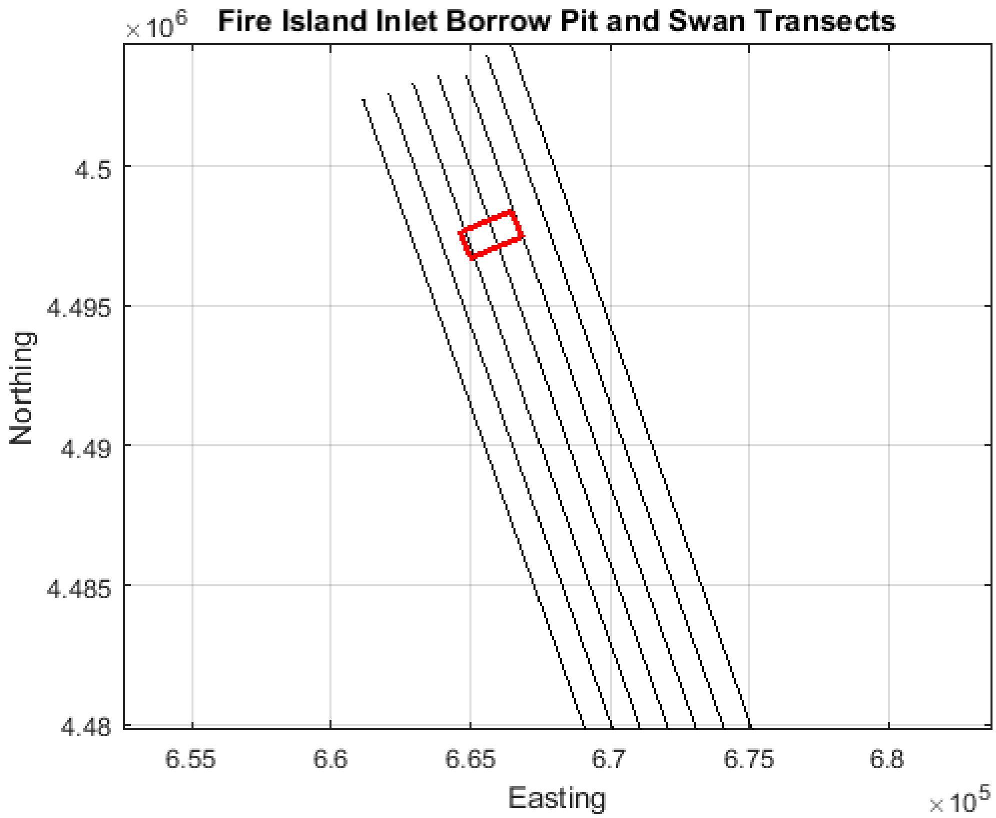

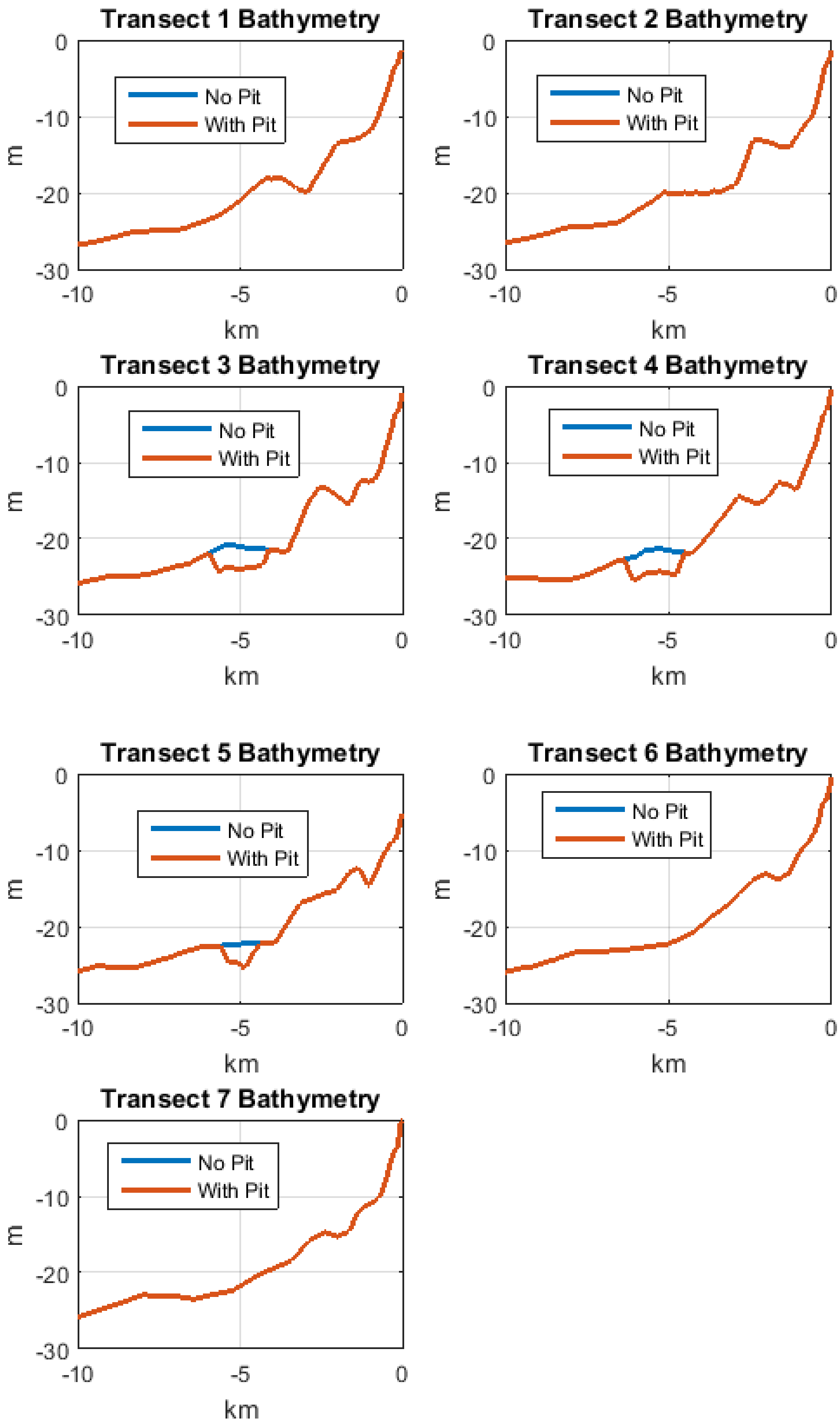

Transect 1 Bathymetry
Transect 2 Bathymetry
Transect 3 Bathymetry
Transect 4 Bathymetry
Transect 5 Bathymetry
Transect 6 Bathymetry
Transect 7 Bathymetry
No Pit
With Pit
m
km
0
-10
-20
-30
-10
-5
0

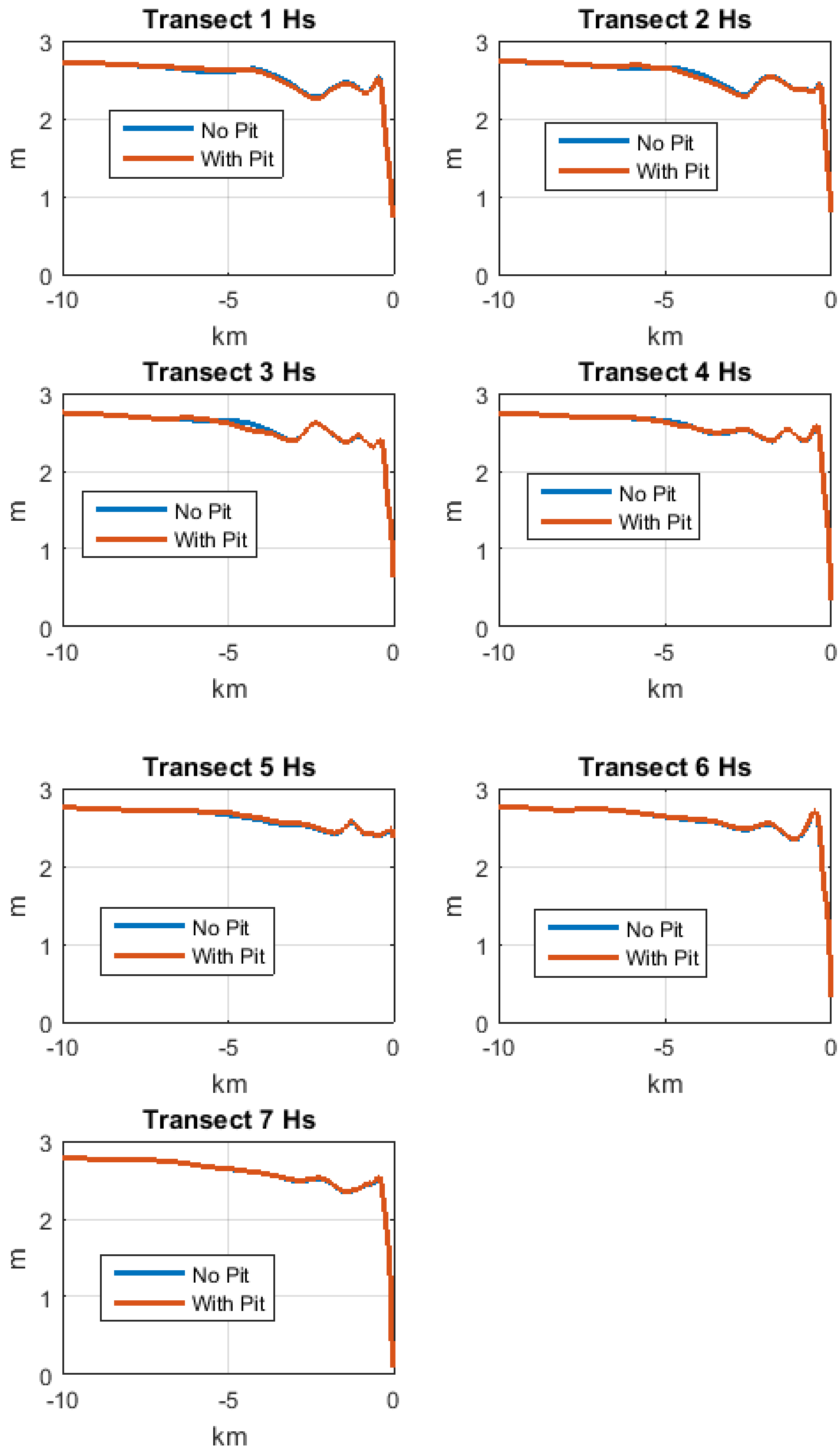
Transect 1 Hs
Transect 2 Hs
Transect 3 Hs
Transect 4 Hs
Transect 5 Hs
Transect 6 Hs
Transect 7 Hs
No Pit
With Pit
m
km
0
1
2
3
-10
-5
0

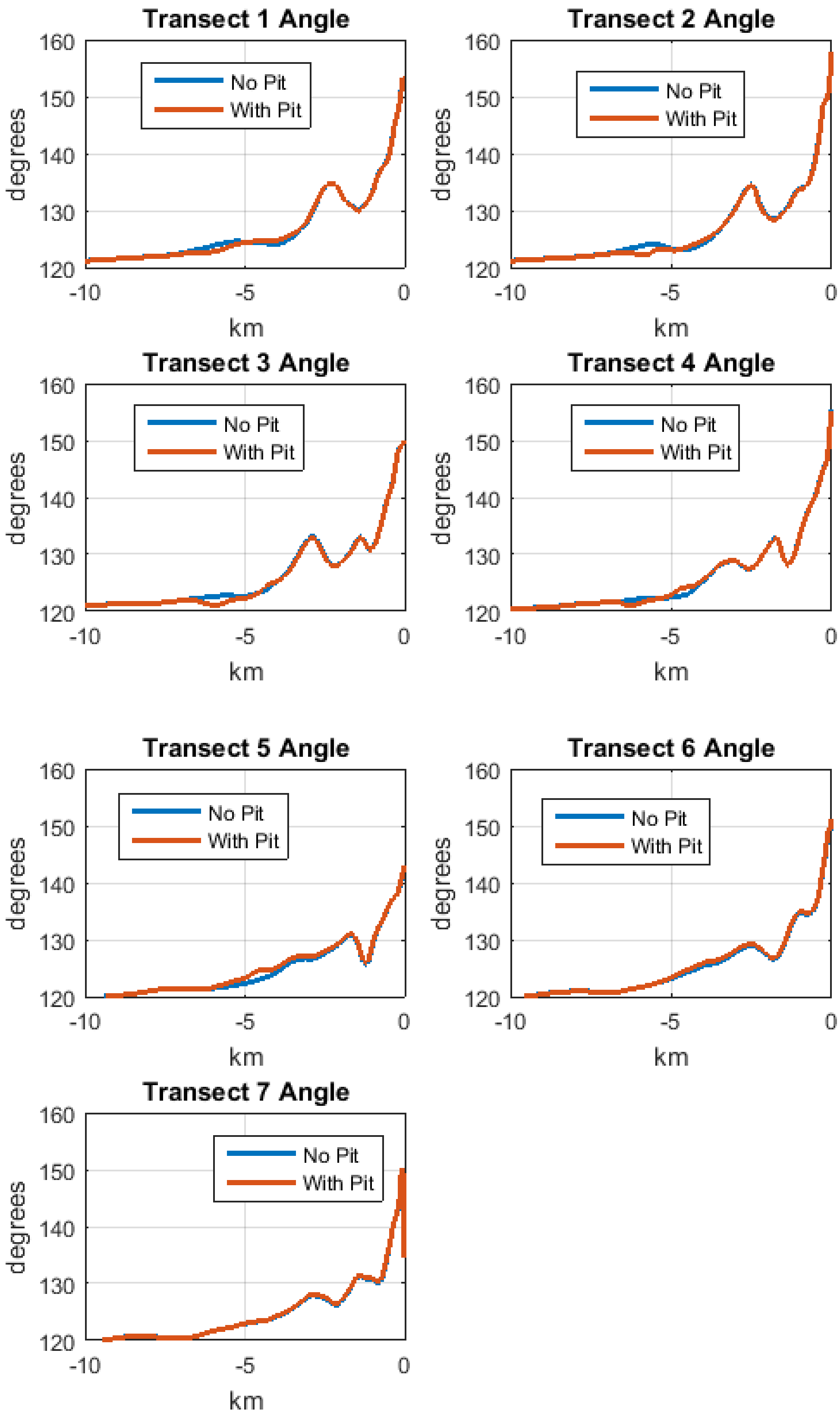
Transcect 1 Angle
Transect 2 Angle
Transect 3 Angle
Transect 4 Angle
Transect 5 Angle
Transect 6 Angle
Transect 7 Angle
No Pit
With Pit
degrees
km
160
150
140
130
120
-10
-5
0

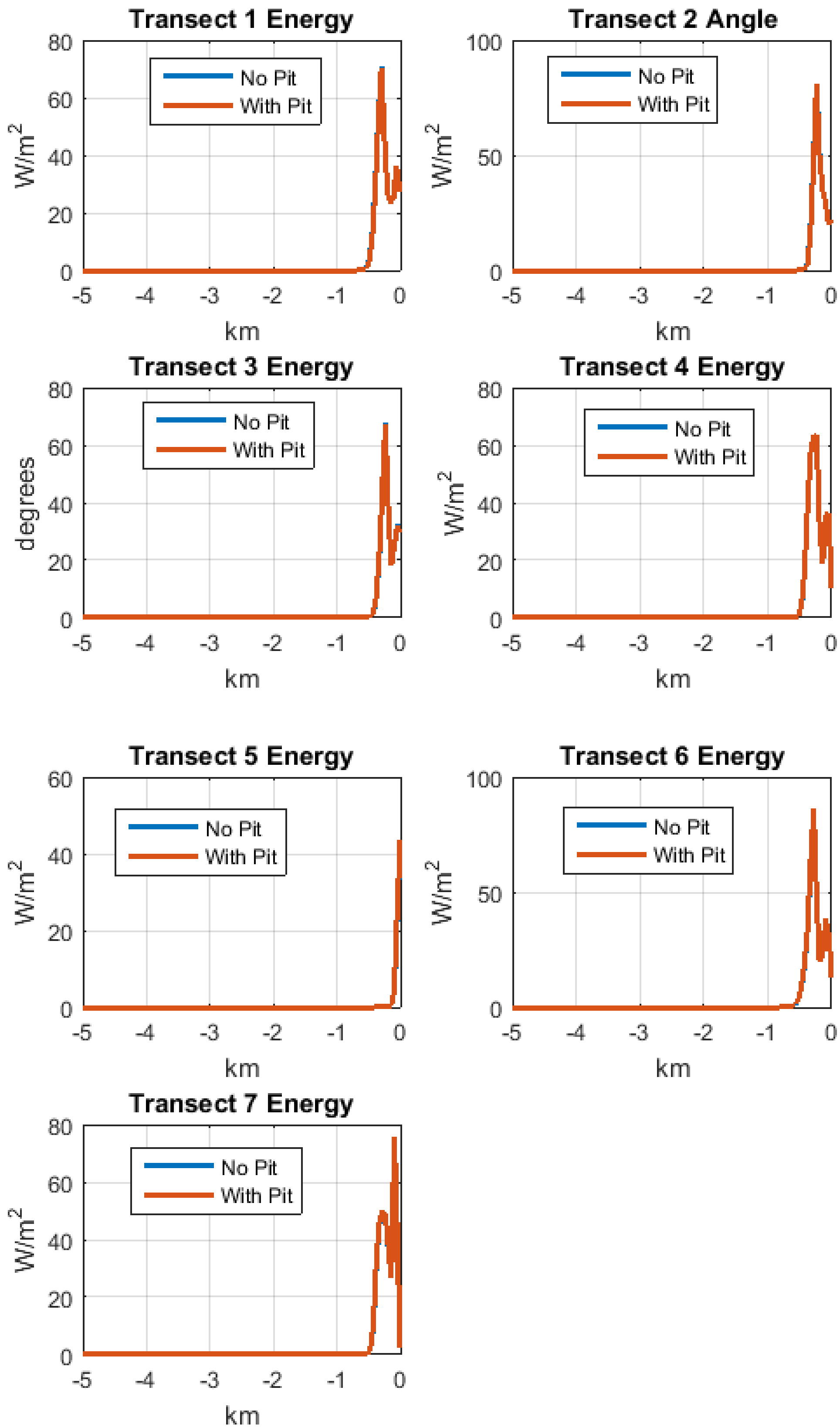
Transect 1 Energy
No Pit
With Pit
W/m^2
km
Transect 2 Angle
No Pit
With Pit
W/m^2
km
Transect 3 Energy
No Pit
With Pit
degrees
km
Transect 4 Energy
No Pit
With Pit
W/m^2
km
Transect 5 Energy
No Pit
With Pit
W/m^2
km
Transect 6 Energy
No Pit
With Pit
W/m^2
km
Transect 7 Energy
No Pit
With Pit
W/m^2
km